Characterization and Use of Acid-Activated Montmorillonite-Illite Type of Clay for Lead(II) Removal

John U. Kennedy Oubagaranadin
Dept. of Ceramic and Cement Technology, PDA College of Engineering, Gulbarga 585102, Karnataka, India
Dept. of Chemical Engineering, S.V. National Institute of Technology, Surat 395007, Gujarat, India

Z. V. P. Murthy
Dept. of Chemical Engineering, S.V. National Institute of Technology, Surat 395007, Gujarat, India

DOI 10.1002/aic.12164
Published online January 20, 2010 in Wiley Online Library (wileyonlinelibrary.com).

The natural local deposits of montmorillonite-illite type of clay (MIC) were susceptible for acid activation. Raw clay was taken for experimentation, disintegrated on acid activation with sulfuric acid, which showed a particle size distribution. The montmorillonite and illite phases in the raw clay disappeared on acid activation and the activated clay, MIC(AA), showed with sodium-aluminum-silicate and beidellite phases apart from quartz (low) phase. The raw and acid-activated clays were characterized using X-ray powder diffractometry, X-ray fluorescence, Fourier transform infrared spectrometry, and energy dispersive X-ray, and their adsorption capacities were compared. When tested for adsorption of Pb(II) in aqueous solutions, the acid-activated clay showed about 50% increased adsorption than raw clay. Sips adsorption isotherm and pseudo-second-order kinetic models were found to be best for the batch adsorption data. Kinetic studies showed the existence of film diffusion and intraparticle diffusion. A two-stage batch adsorber was designed for the removal of Pb(II) from aqueous solutions. © 2010 American Institute of Chemical Engineers *AIChE J,* 56: 2312–2322, 2010
Keywords: adsorption, lead, acid activated clay, isotherm models

Introduction

Clays are basically alumino-silicate minerals containing sodium, potassium, and calcium, in which magnesium and iron may be substituted for aluminum. Some of the clays have adsorption properties. Montmorillonite type of clay can be activated by hydrothermal, ultrasonic, and microwave treatments and its adsorption property improved.[1] Activation of clays can be carried out by calcination, reaction with mineral acids, or a combination of both techniques.

Correspondence concerning this article should be addressed to Z. V. P. Murthy at zvpm2000@yahoo.com.

During calcination process, the water in the clay mineral is driven out as the temperature is increased leaving in its place a porous structure with increased surface area. As the temperature rises up to 500–700°C, the structure is modified and the OH—O bonds are destroyed with the resultant structure having higher adsorptive properties. However, higher temperatures may alter or destroy the structure.

Acid treatment of clays changes the clay structure by creating new pores resulting in an increase of surface acidity through the replacement of cations[2] like Al^{3+}, Fe^{3+}, and Ca^{2+} from the structure with H^{+}. During clay activation with mineral acids, two basic reactions occur. The acid first dissolves part of Al_2O_3 as well as CaO and MgO from the lattice. This causes an opening of the crystal lattice and an

Table 1. Literature for the Removal of Heavy Metals by Clays

Clay	Metal Removed	Adsorption Capacity (mg/g)	Ref.
China clay	Pb^{2+}	0.40	7
Wollastonite	Pb^{2+}	1.70	7
Kaolinite	Zn^{2+}	1.25	8
	Pb^{2+}	0.12	9
	Cd^{2+}	0.32	9
Bentonite	Cd^{2+}	11.41	10
	Zn^{2+}	4.54	10
	Sr^{2+}	32.94	11
	Cr^{3+}	4.29	12
Ball clay	Cd^{2+}	2.24	13
	Cr^{3+}	3.60	13
	Cu^{2+}	1.60	13
	Ni^{2+}	0.41	13
	Zn^{2+}	2.88	13

increase in internal surface area. The second reaction is the gradual exchange of the Ca^{2+} and Mg^{2+} ions located at the surface of the crystal against hydrogen ions from the mineral acid. Acid-activated clay is almost saturated with H^+ ions and exhibits strong acidic character. Activation of clay can be performed using any mineral acid, but activation with hydrochloric or sulfuric acid is most common.

High levels of exposure to Pb may result in toxic biochemical effects in humans, which in turn cause problems in the synthesis of hemoglobin, effects on the kidneys, gastrointestinal tract, joints, and reproductive system, and acute or chronic damage to the nervous system.[3,4] The permissible limit for Pb(II) in the drinking water approved by World Health Organization (WHO)[5] is 0.05 mg/L. In recent years, the adsorption of Pb(II) by clay minerals as adsorbents has led to some work[6,7] on their adsorption properties for Pb(II). Earlier works reported in literature[8–14] for the removal of heavy metals using different types of clays are given in Table 1.

The present work deals with the activation of local Gulbarga clay (a montmorillonite-illite type of clay) by reaction with sulfuric acid and testing its adsorption capacity for Pb(II) from aqueous solutions. The adsorption capacity of

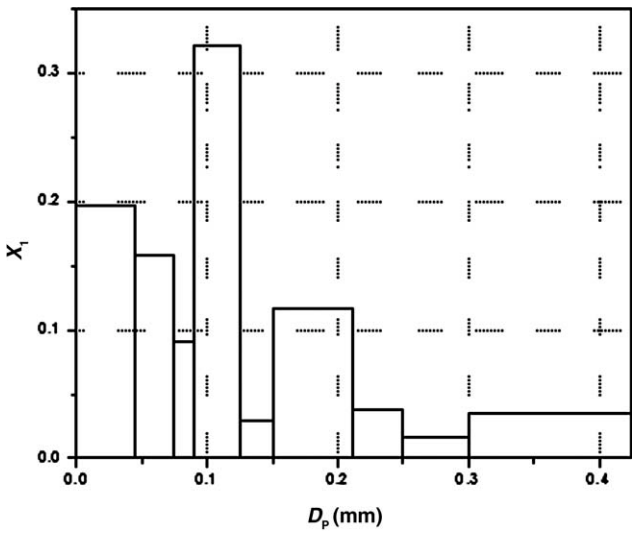

Figure 1. Differential particle size analysis of MIC(AA).

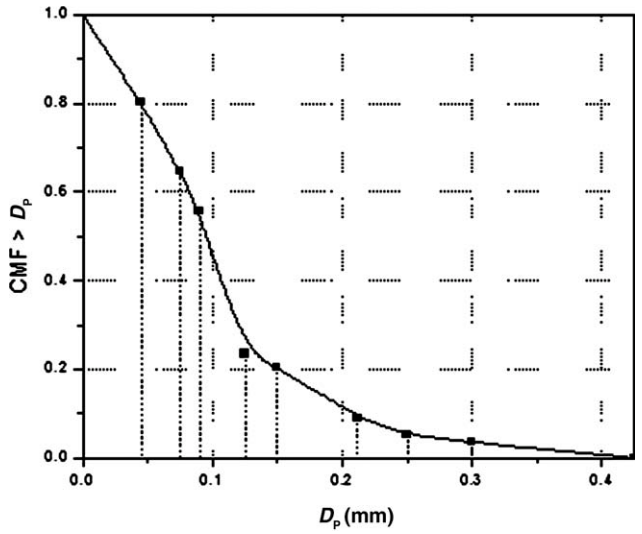

Figure 2. Cumulative particle size analysis of MIC(AA).

acid activated clay and raw clay were compared. The clays were characterized using powder X-ray diffractometry (XRD), X-ray fluorescence (XRF), Fourier transform infrared (FTIR) spectrometry, and energy dispersive X-ray (EDXR) analysis. Also, adsorption data were interpreted with different isotherm and kinetic models.

Materials and Methods

Reagents

All the reagents used in this study were of analytical grade. Nitric acid (HNO_3), sulfuric acid (H_2SO_4), hydrochloric acid (HCl), and sodium hydroxide (NaOH) were obtained from Merck, India. All the glasswares used were immersed overnight in 10% (v/v) nitric acid and rinsed several times with distilled water before use. For adjusting the pH of the medium, 0.1 N solutions of NaOH and HNO_3 were used.

Chemical activation of the adsorbent

A raw clay sample was collected from the mines in the Korvi village of Gulbarga district, Karnataka, India. It was

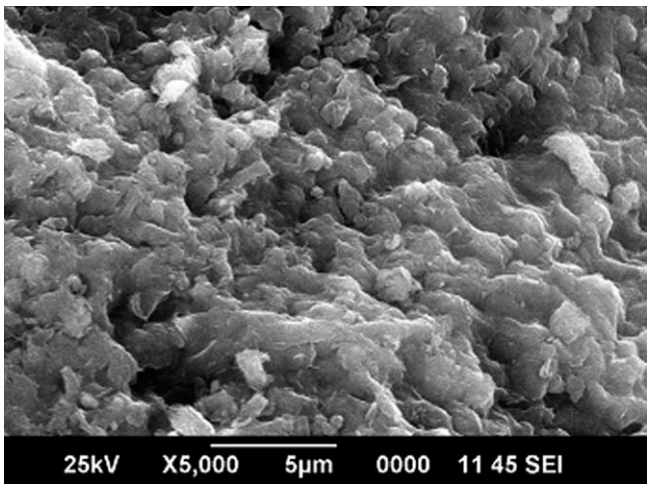

Figure 3. SEM of acid activated MIC.

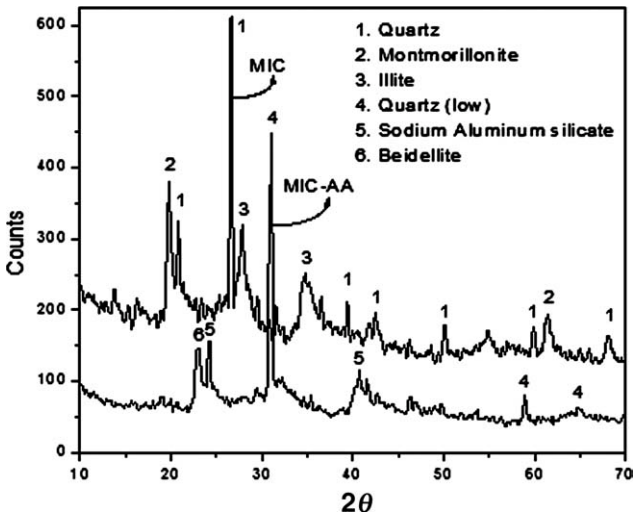

Figure 4. XRD patterns of MIC and MIC(AA).

then ground in a ball mill and sorted into different sized fractions. The clay fraction in the particle size range 425–212 μm was taken for this experimental work. Clay (20 g) was mixed with 400 mL of H_2SO_4 solution, which had 45% of H_2SO_4 by mass of clay. The acid activation of the clay was performed by heating for 6 h in a shaking water bath at 97°C with reflux condensing of the vapors.[15] The activated-clay sample was then washed several times with distilled water to remove sulfate ions. The sample was then dried in an air oven for 24 h at 105°C. The dried sample was then stored in air tight polythene sachets for further experimental work. To identify the different phases in the raw and acid-activated clay, powder XRD was performed. Further characterization of the raw and activated clay was done by XRF and FTIR spectroscopy. Properties of the adsorbents such as specific gravity, pH, and loss on ignition were determined by standard procedures.[16] Differential and cumulative particle size analysis of the clay powder was carried out using standard test sieves. The particle size of a particular sieved fraction was taken as the arithmetic average.

Adsorption experiments and analytical methods

All the adsorption experiments were conducted at the room temperature (28 ± 2°C). Lead nitrate was used as a source of Pb(II) in aqueous solutions. Batch equilibrium studies were conducted with three initial Pb(II) concentrations of 100, 150, and 200 ppm at an initial solution pH of 4, which is favorable for Pb(II) removal.[17] Varying amounts of the raw and acid-activated clay were added to 50 mL Pb(II) solutions in a series of stoppered bottles and shaken on a rotary shaker for 2 h to attain equilibrium. The residual Pb(II) concentrations were then determined with a Pb-ion–selective electrode (pH Products Company, Hyderabad, India).

Kinetic experiments were also carried out at the room temperature for three initial Pb(II) concentrations of 100, 150, and 200 ppm at an initial solution pH of 4. Raw (0.25 g) and acid-activated (0.2 g) clay were separately added to 100 mL Pb(II) solution contained in stoppered bottles and shaken at different time intervals. Vacuum filtration, using a G4 sintered porous funnel, was employed to remove the adsorbent from the solution after each time interval. The residual Pb(II) concentration in the filtrate was determined using Pb-ion–selective electrode.

Isotherm and kinetic models

To examine the relationship between adsorbed and aqueous concentration of Pb(II) at equilibrium, adsorption isotherm models such as Freundlich, Langmuir, and Dubinin-Radushkevich were used for fitting the data. The transient behavior of the batch adsorption process at different initial concentrations was analyzed with the help of pseudo-first-order (Lagergren), pseudo-second-order (Ho), first-order, and second-order kinetic models. Intraparticle and film diffusion models were also applied.

Table 2. XRD Phase Analysis—Compounds in MIC and MIC(AA)

Adsorbent	Compounds	Chemical Formula
MIC	1. Quartz	SiO_2
	2. Montmorillonite	$(Na,Ca)_{0.3}(Al,Mg)_2.Si_4O_{10}(OH)_2.xH_2O$
	3. Illite	$KAl_2(Si_3Al)O_{10}(OH)_2$
	4. Quartz (low)	SiO_2
MIC(AA)	5. Sodium Aluminum Silicate	$Na_8Al_4Si_4O_{18}$
	6. Beidellite	$Na_{0.3}Al_2(Si,Al)_4O_{10}(OH)_2.2H_2O$

Table 3. Specifications of MIC and MIC(AA)

Property	MIC	MIC(AA)
Particle size range	212–106 μm	212–106 μm
Average particle size	~160 μm	~160 μm
Specific gravity	2.4	1.78
pH	8	4.15
Langmuir surface area	156 m^2/g	251 m^2/g
Loss on ignition	11.1%	6.94%

Results and Discussion

Particle size distribution

Because of the action of sulfuric acid on the clay during activation process, the clay particles break up into smaller ones and the result is a particle size distribution in the activated clay product.[18] The particle size distribution for the acid activation conditions, adopted in this work, is shown in Figures 1 and 2. Figure 3 shows the Scanning Electron Micrograph (SEM) of MIC(AA) taken with a JEOL model JSM-6390LV instrument. The cumulative mass fraction (CMF) of clay particles, having size greater than the feed

Table 4. Chemical Composition of MIC and MIC(AA)

	Wt %	
Chemical Compound	MIC	MIC(AA)
SiO_2	48.523	53.996
Al_2O_3	9.682	8.937
Fe_2O_3	18.809	14.093
CaO	17.042	16.751
MgO	3.971	2.863
K_2O	1.768	2.265
Na_2O	0.139	0.140
SO_3	0.065	0.955

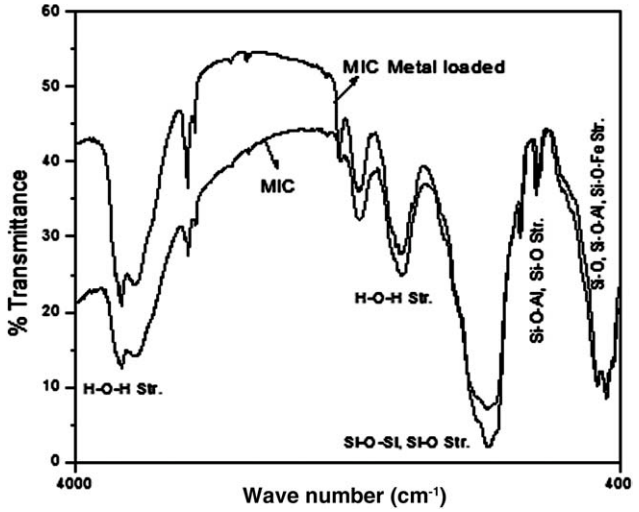

Figure 5. FTIR spectra of MIC and metal loaded MIC.

mean diameter of 0.2125 mm, was about 9%, which indicated that there was considerable disintegration of clay particles during acid activation and increase in external specific surface area of the sample. The external specific surface area of the clay powder of a fixed average particle diameter was calculated using the following equation[19]:

$$A_w = \frac{6}{\phi \rho \overline{D_p}} = 0.0112 \text{ m}^2/\text{g} \quad (1)$$

The acid-activated clay showed a particle size distribution and an external specific surface area (A_w) that is given by:

$$A_w = \frac{6}{\phi \rho} \sum \frac{x_i}{\overline{D_{pi}}} = 80.62 \text{ m}^2/\text{g} \quad (2)$$

where, ρ is the particle density, x_i is the mass fraction, and ϕ is the sphericity (0.7). The considerable increase in the external surface area as given by the numerical values of Eqs. 1, 2 indicated particle disintegration due to acid activation.

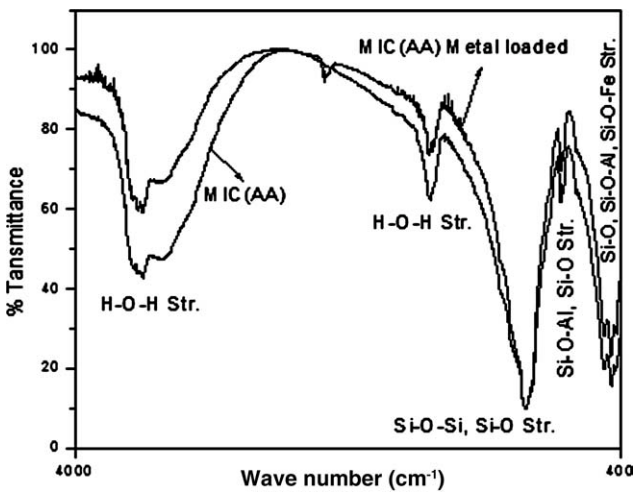

Figure 6. FTIR spectra of MIC(AA) and metal loaded MIC(AA).

Table 5. FTIR Bands of MIC and MIC(AA)

Band (cm^{-1})	Assignments
3437	H—O—H Str.
1651	H—O—H Str.
1030	Si—O—Si, Si—O Str.
775	Si—O, Si—O—Al Str.
460	Si—O, Si—O—Fe Str.

Instrumental analysis characterization

Mineral Phase Analysis. X-ray diffraction is used for material structural and phase analysis. Phase analysis of the MIC and MIC(AA), was carried out with the help of powder XRD (Bruker AXS D8 Advance). Some of calcium, potassium, and magnesium were removed from the MIC as their corresponding sulfates during acid activation, which lead to the disappearance of the montmorillonite and illite phases in MIC(AA). Also there was inversion of quartz to quartz (low) due to acid activation. The superimposed XRD patterns of MIC and MIC(AA) are shown in Figure 4 and the mineral phase compositions are given in Table 2. The physical specification of MIC and MIC(AA) clay adsorbents used in the study are given in Table 3.

Chemical Composition of Clay. XRF was used (ARL/XRF-8600) to know the chemical composition of the adsorbent MIC and MIC(AA). The data are given in Table 4. Significant change in the chemical composition of the clay took place due to acid activation. The proportion of Al_2O_3, Fe_2O_3, CaO, and MgO reduced in MIC(AA) due to their removal by the action of sulfuric acid.

Fourier Transform Infrared Spectrum. The delicate interactions with the surrounding atoms or molecules impose the stamp of individuality of the spectrum of each compound. A Thermo Nicolet, Avatar 370 instrument was used to acquire the FTIR spectrums of MIC and MIC(AA), before and after adsorption. Superimposed FTIR spectrums are shown in Figures 5 and 6. Si—O stretching vibrations were observed at about 775 and 460 cm^{-1} showing the presence of quartz. Band at 3565 cm^{-1} indicated the possibility of the hydroxyl linkage. However, the

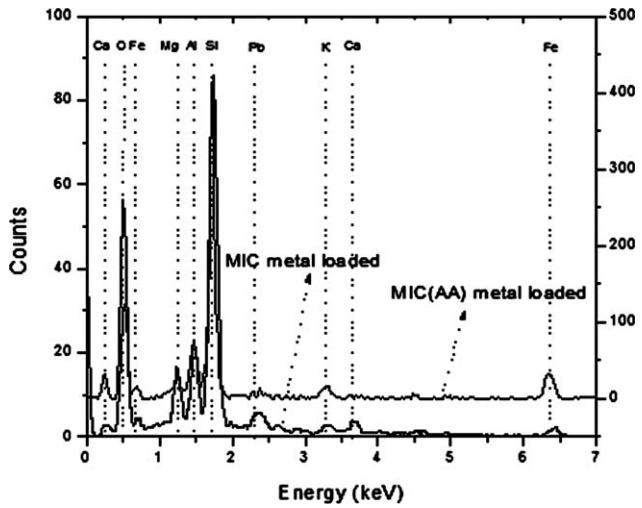

Figure 7. EDXR spectra of metal loaded MIC and MIC(AA).

Table 6. Adsorption Isotherms and Parameter Values

Model	Equation	R^2	χ^2	C_0 (ppm)	MIC			MIC(AA)		
1. Freundlich	$q_e = K_F C_e^{1/n}$	0.9865	4.8290	100	$n = 2.50$; $K_F = 9.11$			$n = 2.74$; $K_F = 15.43$		
				150	$n = 4.31$; $K_F = 19.15$			$n = 3.13$; $K_F = 17.07$		
				200	$n = 4.58$; $K_F = 19.60$			$n = 3.19$; $K_F = 16.38$		
2. Langmuir	$q_e = \frac{q_m K_L C_e}{1+K_L C_e}$	0.9939	2.1929	100	$q_m = 54.12$; $K_L = 0.0783$			$q_m = 87.59$; $K_L = 0.0626$		
				150	$q_m = 54.52$; $K_L = 0.1645$			$q_m = 88.40$; $K_L = 0.0458$		
				200	$q_m = 56.77$; $K_L = 0.1351$			$q_m = 89.29$; $K_L = 0.0356$		
3. D-R	$q_e = q_m \exp(-D\varepsilon^2)$	0.9227	27.6562	100	$q_m = 39.79$; $D = 5.29$ E -6			$q_m = 66.03$; $D = 9.94$ E-6		
				150	$q_m = 46.84$; $D = 3.07$ E-6			$q_m = 70.10$; $D = 4.00$ E-5		
				200	$q_m = 50.09$; $D = 4.86$ E-6			$q_m = 71.62$; $D = 7.00$ E-5		
					q_m	K_{LF}	N	q_m	K_{LF}	N
4. Sips	$q_e = \frac{q_m K_{LF} C_e^N}{1+K_{LF} C_e^N}$	0.9989	0.4878	100	52.75	0.0744	1.0450	92.62	0.0718	0.9077
				150	67.70	0.2398	0.5988	87.43	0.0432	1.0249
				200	109.03	0.1831	0.3612	90.26	0.0378	0.9765

bands at 3437 and 1651 cm^{-1} in the spectrum suggested the possibility of water of hydration in the clay.[20] The FTIR absorption bands and their respective assignments are given in Table 5. Although there was no major change in the IR absorption bands of the adsorbents before and after adsorption, a slight shift in some of the peaks shown by metal loaded MIC and MIC(AA) may be due to the presence of adsorbed Pb.

Energy Dispersive X-ray Analysis. Qualitative elemental analysis was performed on the metal loaded clay adsorbents, to know if the metal Pb(II) was actually removed by adsorption, using a JEOL model JED-2300 EDAX instrument. The EDXR spectrum of the metal loaded clay adsorbents (Figure 7) showed the presence of adsorbed Pb(II) in the clay.

All the aforementioned instrumental characterization services were rendered by Sophisticated Test and Instrumentation Centre, Cochin University of Science and Technology, Kochi, Kerala, India.

Adsorption isotherm analysis

The batch adsorption equilibrium data were tested with Freundlich,[21] Langmuir,[22] Dubinin-Radushkevich,[23] and Sips or Freundlich-Langmuir[24] models. The Freundlich isotherm, which is a multilayer model, is empirical in nature and the Langmuir isotherm, a monolayer model, is an analytical equation, which has proper scientific basis. The model equations, parameters and the values of R^2 and χ^2, which represent goodness-of-fit of experimental data to the models, are given in Table 6. Freundlich and Langmuir models are widely used by researchers to fit batch adsorption equilibrium data. The value of "n," of the Freundlich model falling in the range of 1–10 indicates favorable adsorption,[25] while K_L of Langmuir model is a coefficient attributed to the affinity between the adsorbent and adsorbate. The Dubinin-Radushkevich isotherm is a temperature-independent and a more general model than Freundlich and Langmuir models. It predicts energy of adsorption per molecule of adsorbate. Sips model is a combination of Freundlich and Langmuir models. It represents Langmuir model for the exponent (N) value of "1," and for low values of the exponent it corresponds to Freundlich model. The experimental data for the batch adsorption of Pb(II) on MIC and MIC(AA) were fitted to the aforementioned adsorption isotherm models by simultaneous nonlinear curve-fitting procedure using Origin 6.0® software, Microcal.

Among the two-parameter isotherm models tested, the best fit to the experimental data was provided by the Langmuir model. The Langmuir parameter q_m, indicated a considerable increase in the monolayer adsorption capacity of MIC(AA), about 63% over that of raw MIC (Table 6). This was due to the considerable increase in the specific surface area and active adsorption sites in MIC(AA) due to acid activation. A lesser value of K_L, which represents adsorption energy, for adsorption of Pb(II) on MIC(AA) was due to the acidity (H^+ ion presence) of the adsorbent. The Freundlich model also provided a fair fit to the data. The values of the parameter "n" in between 2 and 5 (Table 6) implied that both MIC and MIC(AA) were good adsorbents[25] for Pb(II). The best fitting three-parameter Sips model is shown in Figure 8. The value of the Sips exponent N close to 1 for MIC(AA) indicated that only monolayer adsorption was possible on it. However, the exponent values for MIC indicated the possibility of multilayer adsorption on it at higher solutions concentrations.

Effect of contact time (kinetic studies)

Pb(II) adsorption onto the clays proceeds in two stages: a fast adsorption process followed by a slow process. Retention of heavy metal ions on clays mainly occurs by ion

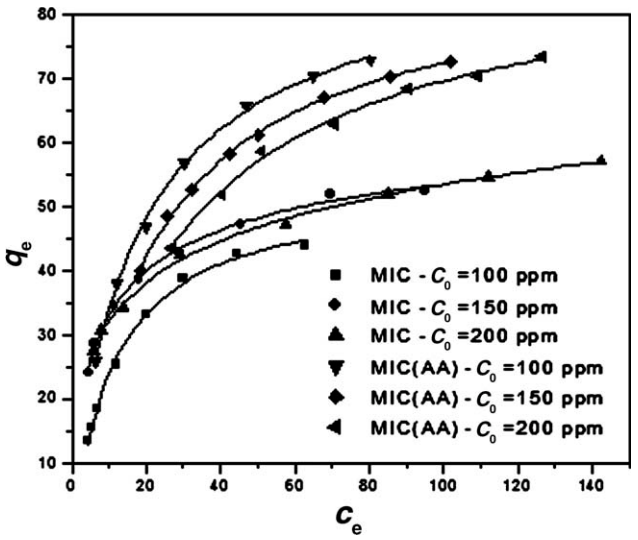

Figure 8. Sips plots.

Table 7. Kinetic Models and Parameter Values

Model	Equation	R^2	χ^2	C_0 (ppm)	MIC	MIC(AA)
1. Pseudo-first-order (Lagergren)	$q_t = q_e\,(1 - e^{-k_1 t})$	0.9856	2.3181	100	$q_e = 15.83$; $k_1 = 1.065$	$q_e = 36.05$; $k_1 = 0.3448$
				150	$q_e = 18.65$; $k_1 = 0.812$	$q_e = 35.37$; $k_1 = 0.2504$
				200	$q_e = 29.50$; $k_1 = 0.062$	$q_e = 33.85$; $k_1 = 0.1318$
2. Pseudo-second- order (Ho)	$q_t = \frac{q_e^2 k_2 t}{1+q_e k_2 t}$	0.9946	0.8802	100	$q_e = 16.88$; $k_2 = 0.1097$	$q_e = 38.37$; $k_2 = 0.0166$
				150	$q_e = 20.14$; $k_2 = 0.0571$	$q_e = 38.19$; $k_2 = 0.0110$
				200	$q_e = 34.79$; $k_2 = 0.0021$	$q_e = 38.12$; $k_2 = 0.0046$
3. First-order	$C_t = C_0 \exp(-k_f t)$	0.7569	575.13	100	$k_f = 0.0293$	$k_f = 0.1004$
				150	$k_f = 0.0162$	$k_f = 0.0191$
				200	$k_f = 0.0073$	$k_f = 0.0089$
4. Second-order	$C_t = \frac{C_0}{(C_0 k_s t+1)}$	0.8449	367.02	100	$k_s = 0.00060$	$k_s = 0.00175$
				150	$k_s = 0.00015$	$k_s = 0.00024$
				200	$k_s = 0.00005$	$k_s = 0.00007$

exchange.[26] Pb(II) ions can also be adsorbed by the silanol groups (Si—OH). The process can be represented as:

$$\text{Clay mineral } M^{n+} + Pb^{2+} \leftrightarrow \text{Clay mineral } Pb^{2+} + M^{n+}\ [M : Na, K, Ca, Mg.\ etc.] \quad (3)$$

$$Si - OH + Pb^{2+} \leftrightarrow Si - OPb^{+} + H^{+} \quad (4)$$

$$2Si - OH + Pb^{2+} \leftrightarrow (Si - O)_2 Pb + 2H^{+} \quad (5)$$

Rate Constant Study. The adsorption kinetics, in general, include two phases: a rapid removal stage followed by a much slower stage before the equilibrium is established. The rate constant for surface adsorption of the Pb(II) ions on MIC and MIC(AA) was studied with the help of the pseudo-first-order-Lagergren rate model[27] and the pseudo-second-order Ho's rate model.[28] The model equations and their parameter values are given in Table 7. The best fit to the kinetic data for the adsorption of Pb(II) on MIC and MIC(AA) was provided by the pseudo-second-order model as indicated by the values of R^2 and χ^2 (Figure 9). Hence, the rate of adsorption of Pb(II) on these adsorbents was of pseudo-second-order. A lower value of the pseudo-kinetic constant for MIC(AA) when compared to that of raw MIC can be attributed to its acidic nature. To understand the variation in the values of kinetic constants for the adsorption of Pb(II) on MIC and MIC(AA), first-order and second-order reaction rate models[29] were tested to the kinetic data. The increase in the reaction rate constant (first-order and second-order) with decreasing pH of the adsorbent indicated an acid catalyzed reaction (Table 7). As MIC(AA) was acidic, the adsorption of Pb(II) on it was catalyzed by H^+ ions.

Mass Transfer Study: Intraparticle Diffusion (IPD). The adsorbate transport from the solution phase to the surface of the adsorbent particles occurs in several steps. The overall adsorption process may be controlled either by one or more steps, e.g., film or external diffusion, pore diffusion, surface diffusion and adsorption on the pore surface, or a combination of more than one step. Besides adsorption at the outer surface of the adsorbent, there is also a possibility of intraparticle diffusion of the metal ion from the bulk of the outer surface into the pores of the adsorbent material, which is usually a slow process. The possibility of intraparticle diffusion can be studied using the intraparticle diffusion model[30–33]:

$$q_t = k_{ip}\sqrt{t} + I \quad (6)$$

where, k_{ip} is the intraparticle diffusion rate constant and I is a constant that gives idea about the thickness of the boundary layer; i.e., larger the value of "I," the greater is the boundary

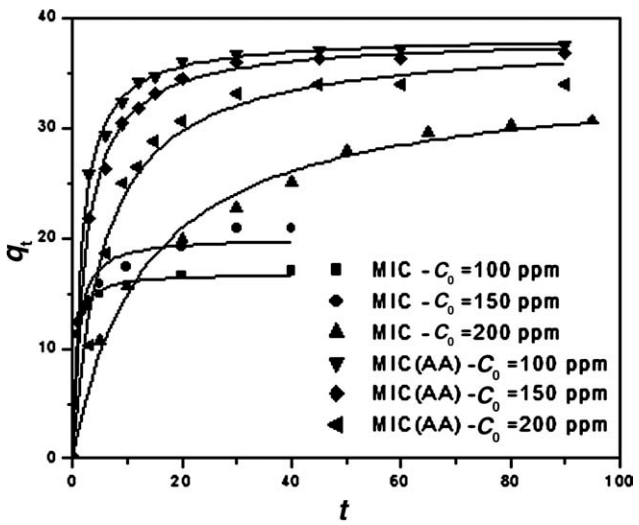

Figure 9. Pseudo-second-order kinetic plots.

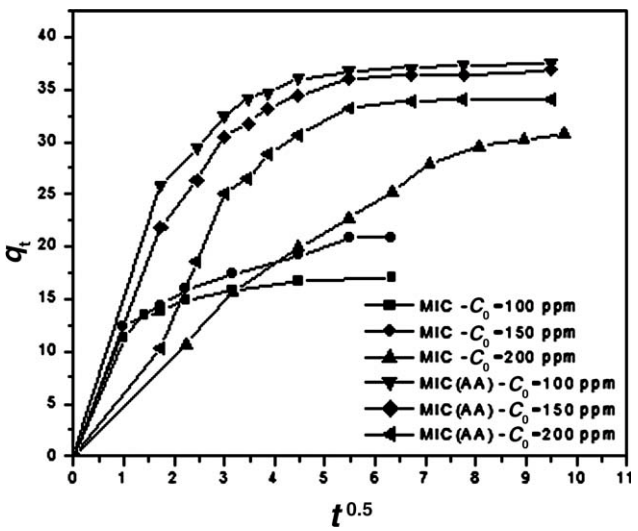

Figure 10. Multilinearity of kinetic data.

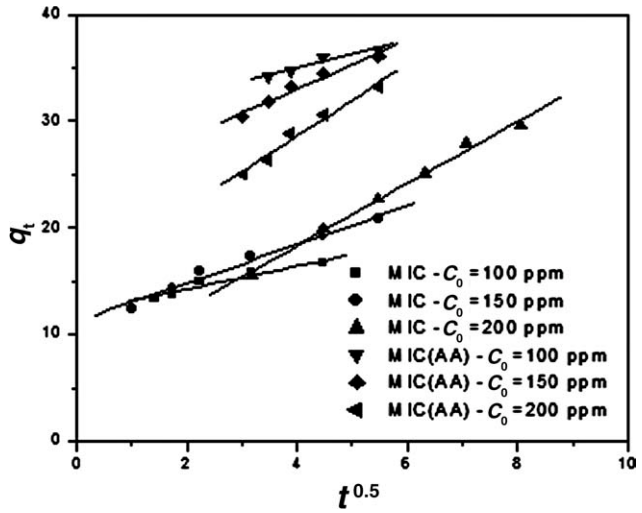

Figure 11. Intraparticle diffusion plots (IPD-1).

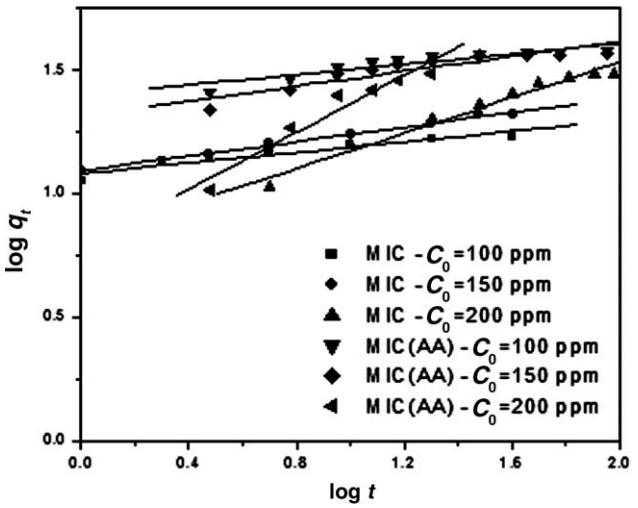

Figure 12. Intraparticle diffusion plots (IPD-2).

layer effect.[34] If the Weber-Morris plot of q_t vs. $\sqrt{t}$ gives a straight line, then the adsorption process is controlled by intraparticle diffusion only. However, if the data exhibit multilinear plots, then two or more steps influence the adsorption process.

When intraparticle diffusion plays a significant role in controlling the kinetics of the adsorption process,[35–39] the plots of q_t vs. $\sqrt{t}$ yield straight lines passing through the origin and the slope gives the rate constant k_{ip}. This plot for the adsorption of Pb(II) on MIC and MIC(AA) showed multilinearity (Figure 10). The multilinearity indicated that multiple mass transfer steps are occurring. The first, linear portion is ascribed to the diffusion of adsorbate through the solution to the external surface of adsorbent or the boundary layer (film) diffusion of solute molecules. The second portion describes the gradual adsorption stage, as the adsorbate diffuses through the pores of the adsorbent, where intraparticle diffusion is rate limiting. The third portion is attributed to the final equilibrium stage for which the intraparticle diffusion starts to slow down due to the very low adsorbate concentration left in the solution. The plot in Figure 11 (IPD-1) shows the intraparticle diffusion ranges for the adsorbents. The values of the intraparticle diffusion constant for the adsorption of Pb(II) on MIC and MIC(AA) are given in Table 8. The increase in the value of k_{ip} (Table 8) was justified since there was an increase in the concentration driving force.

Further confirmation to the occurrence of intraparticle diffusion was obtained from a plot of log (q_t) vs. log (t) (IPD-2) as shown in Figure 12. The plots gave nearly a linear fit indicating intraparticle diffusion taking place. The values of the slope calculated from the plots are given in Table 8. A value of 0.5 corresponds to the intraparticle diffusion being nearly rate determining. The divergence in value from 0.5 indicates that besides intraparticle diffusion, there may be other processes controlling the rate, all-operating at the same time.

Film Diffusion Studies. When the transport of the solute molecules from the liquid phase to the solid phase boundary plays significant role in adsorption, the liquid film diffusion model[40] can be applied, which is given as:

$$\ln(1 - F) = -k_{fd}t \tag{7}$$

where, F is the fractional attainment of equilibrium ($F = q_t/q_e$), and k_{fd} is the film diffusion rate constant. A linear plot of $-\ln(1 - F)$ vs. t with zero intercept would propose that the kinetics of the adsorption process is primarily controlled by diffusion through the liquid film surrounding the solid adsorbent. This plot is shown in Figure 13. The straight lines are not passing through the origin for 100 and 150 ppm solutions and so the adsorption process is not primarily film diffusion controlled. The intercept is almost 0 [i.e. 0.0085 for MIC and 0.0081 for MIC(AA)] for 200 ppm solution and

Table 8. Mass Transfer Constants for the Adsorption of Pb(II) on MIC and MIC(AA)

		MIC		MIC(AA)	
Plot	C_0 (ppm)	Slope	Intercept	Slope	Intercept
$q_t = k_{ip} \cdot \sqrt{t} + 1[IPD - 1]$	100	$k_{ip} = 1.07$	$I = 12.12$	$k_{ip} = 1.31$	$I = 29.78$
	150	$k_{ip} = 1.79$	$I = 11.27$	$k_{ip} = 2.26$	$I = 23.98$
	200	$k_{ip} = 2.90$	$I = 6.76$	$k_{ip} = 3.36$	$I = 15.22$
log q_t vs. log t [IPD-2]	100	0.106		0.105	
	150	0.146		0.147	
	200	0.358		0.309	
$ln(1 - F) = -k_{fd} \cdot t$ [Film diffusion]	100	$k_{fd} = 0.1588$	0.9057	$k_{fd} = 0.0323$	0.4915
	150	$k_{fd} = 0.1572$	0.3867	$k_{fd} = 0.0301$	0.4087
	200	$k_{fd} = 0.0509$	0.0085	$k_{fd} = 0.0542$	0.0081

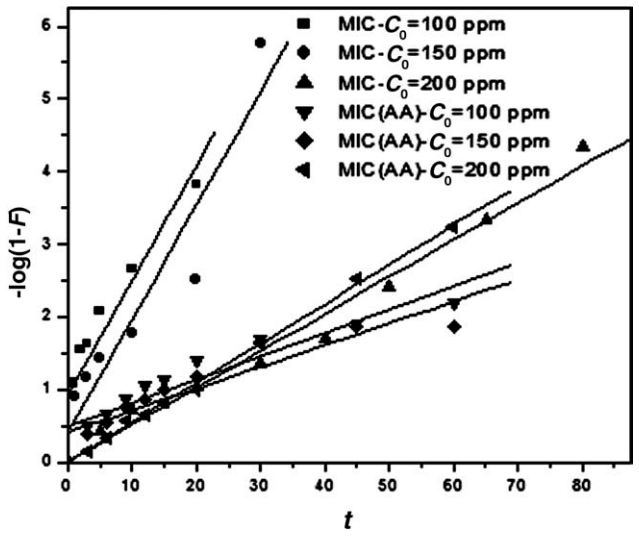

Figure 13. Film-diffusion plots.

hence in this case it is film diffusion controlled. The film diffusion rate constants k_{fd}, calculated from the slopes are given in Table 8. Error estimates at 95% confidence level for all the fitted parameters are given in Table 9.

External Mass Transfer Coefficient. According to the typical adsorption model[41,42] for describing the process, an expression for the external mass transfer coefficient can be given as[43]:

$$k_e = \frac{mk_2 q_e^2}{C_0 A_s} \tag{8}$$

where, k_e is the external mass transfer coefficient (cm/s); m is the mass of the adsorbent (g), k_2 is the second-order kinetic rate constant (g/mg s); q_e is the equilibrium metal uptake by the adsorbent (mg/g); C_0 is the initial Pb(II) concentration of the solution (mg/cm^3), and A_s is the external surface area of the adsorbent particles (cm^2). A_s is given by the following equation:

$$A_s = \frac{6m}{\phi \rho v_p} \tag{9}$$

where, v_p is the particle volume. The values of the calculated external mass transfer coefficients for the adsorption of Pb(II) on MIC and MIC(AA) are given in Table 10. The reciprocal of k_e is a measure of the resistance to mass transfer. These values of external mass transfer coefficient are comparable to the values available in literature for the adsorption of Pb(II) on clays.[44]

Design of batch adsorber

The two-parameter Langmuir isotherm model was used to design a two-stage adsorber for adsorbent optimization. The solution to be treated contains V (L) of Pb(II) solution of initial concentration C_0 ppm. The Pb(II) concentration is to be reduced from C_{n-1} ppm to C_n ppm. W(g) of adsorbent with solid phase concentration of q_0 is used to reduce the Pb(II) concentration and Pb(II) adsorbed on the adsorbent increases from q_0 to q_n (mg/g). The metal uptake can be represented by a mass balance equation:

$$V(C_{n-1} - C_n) = W(q_n - q_0) \tag{10}$$

Rearrangement of Eq. 10 gives,

$$q_n = \frac{V}{W}(C_{n-1} - C_n) \tag{11}$$

If the equilibrium metal uptake follows Langmuir isotherm model, then

$$q_n = \frac{q_m K_L C_n}{1 + K_L C_n} \tag{12}$$

Table 9. Error Estimates (±) for Fitted Parameters (95% Confidence Level)

			Error Estimates					
			MIC			MIC(AA)		
Sl. No.	Model	Fitted Parameter	C_0 = 100 ppm	C_0 = 150 ppm	C_0 = 200 ppm	C_0 = 100 ppm	C_0 = 150 ppm	C_0 = 200 ppm
1	Freundlich	n	0.1968	0.3721	0.3702	0.1627	0.2448	0.2874
		K_F	0.9875	1.3963	1.4200	1.2652	1.7157	2.0000
2	Langmuir	q_m	2.0011	1.1286	0.9844	2.0077	2.2498	2.4285
		K_L	0.0081	0.0147	0.0111	0.0045	0.0037	0.0033
3	D-R	q_m	2.7077	2.3663	2.3231	2.6600	2.9014	3.0418
		D	1.27E−6	7.99E−7	1.19E−6	1.93E−6	7.78E−6	2.00E−5
4	Sips	q_m	2.2904	4.5942	28.1636	3.6398	3.9406	5.5139
		K_{LF}	0.0075	0.0122	0.0417	0.0059	0.0105	0.0126
		N	0.0748	0.0650	0.0619	0.0545	0.1032	0.1291
5	Lagergren	q_e	0.7281	0.6871	0.8539	0.5793	0.6266	0.7572
		k_1	0.2611	0.1753	0.0067	0.0350	0.0228	0.0106
6	Ho	q_e	0.5866	0.5526	0.9341	0.4993	0.5419	0.6979
		k_2	0.0300	0.0117	0.0003	0.0019	0.0011	0.0004
7	First-order	k_f	0.01260	0.00485	0.00127	0.03040	0.00381	0.00170
8	Second-order	k_s	0.00024	0.00004	8.24E-6	0.00059	0.00005	0.00001
9	IPD-1	k_{ip}	0.1878	0.1218	0.1167	0.3065	0.2416	0.2416
		I	0.5311	0.4131	0.6986	1.3446	1.0020	1.0020
10	IPD-2	Slope	0.0309	0.0302	0.0354	0.0309	0.0309	0.0309
11	Film diffusion	k_{fd}	0.0192	0.0121	0.0042	0.0057	0.0057	0.0057
		Intercept	0.1681	0.1726	0.1789	0.1543	0.1543	0.1543

Table 10. External Mass Transfer Coefficient, k_e

		MIC				MIC(AA)			
C_0 (ppm)	C_0 (mg/cm^3)	k_2 (g/mg s)	q_e (mg/g)	k_e (cm/s)	$1/k_e$ (s/cm)	k_2 (g/mg s)	q_e (mg/g)	k_e (cm/s)	$1/k_e$ (s/cm)
100	0.10	1.828×10^{-3}	16.88	3.129×10^{-6}	3.196×10^{5}	2.770×10^{-4}	38.37	1.817×10^{-6}	5.503×10^{5}
150	0.15	9.517×10^{-4}	20.14	1.546×10^{-6}	6.468×10^{5}	1.837×10^{-4}	38.19	7.959×10^{-7}	1.256×10^{6}
200	0.20	3.667×10^{-5}	34.79	1.334×10^{-7}	7.496×10^{6}	7.700×10^{-5}	38.12	2.493×10^{-7}	4.011×10^{6}

Combining Eqs. 10 and 11, the amount of adsorbent required for the desired metal removal can be predicted as

$$W = \frac{V(C_{n-1} - C_n)(1 + K_L C_n)}{q_m K_L C_n} \tag{13}$$

The design objective was to treat 50 L of 200 ppm Pb(II) solution in the first stage. A series of equilibrium metal concentrations from 180 ppm to 20 ppm in nine decrements was considered in stage 1 of a two-stage adsorption system. In the adsorption system 1, the design objective was to reduce the initial metal concentration from 200 to 180 ppm. Similarly, in the adsorption system 2, 3, 4, 5, 6, 7, 8, and 9, the design objective of the first stage was to reduce the initial metal concentration from 200 to 160, 140, 120, 100, 80, 60, 40, and 20 ppm, respectively. For all the adsorption systems, the design objective of the second stage was to reduce the equilibrium metal concentration in stage 1 to 20 ppm. The corresponding amount of adsorbent needed for the required amount of metal removal in stage 1 and stage 2 were calculated using Eq. 13. Based on the adsorption system number that utilized, the minimum adsorbent dose to reduce the metal concentration from C_{n-1} to C_n ppm, the optimum dose was predicted from the plot of total adsorbent dose required in both stages of two-stage adsorption system vs. the equilibrium concentration in stage 1 (see Figure 14). It was observed that the seventh two-stage adsorption with equilibrium concentration 60 ppm in stage 1 utilized minimum mass of the adsorbent MIC and MIC(AA) to achieve the desired objective of reducing 50 L of metal solution from 200 to 20 ppm Pb(II) concentration.

A similar two-stage adsorption system was developed for a 100 L solution volume for decreasing the initial Pb(II) concentration from 200 to 20 ppm. The minimum amount of the adsorbent required for different volumes of metal solution to be treated was calculated from the plot on total amount of adsorbent required at both the stages vs. adsorption system number for different volumes of Pb(II) solution (see Figure 15). The predicted optimized adsorbent required for two-stage adsorption system to reduce the metal concentration from 200 to 20 ppm for different metal solution volumes is given Table 11. It was observed that a two-stage adsorption system reduced the MIC and MIC(AA) adsorbents dose by about 14 and 30%, respectively, when compared with that of single-stage adsorption system.

Conclusions

Powder XRD pattern of the adsorbent MIC indicated that it primarily consisted of quartz, montmorillonite, and illite mineral phases. However, after acid treatment, the montmorillonite and illite phases disappeared. This was due to the removal of some amount of Fe, Ca, Mg, and Al from the clay in the form of their respective sulfates due to the action of sulfuric acid. Isotherm studies revealed multilayer adsorption on the MIC adsorbent and monolayer adsorption on MIC(AA). The monolayer adsorption capacity for Pb(II) was found to be about 54 and 88 mg/g for MIC and MIC(AA), respectively. There was about 63% increase in the monolayer adsorption capacity of the clay adsorbent due to acid activation. This was due to the increase in the surface area

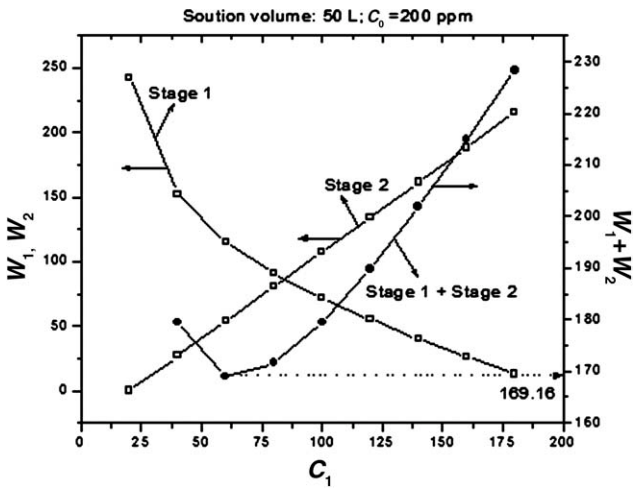

Figure 14. Optimization of MIC(AA) dosage in a two-stage batch adsorption system.

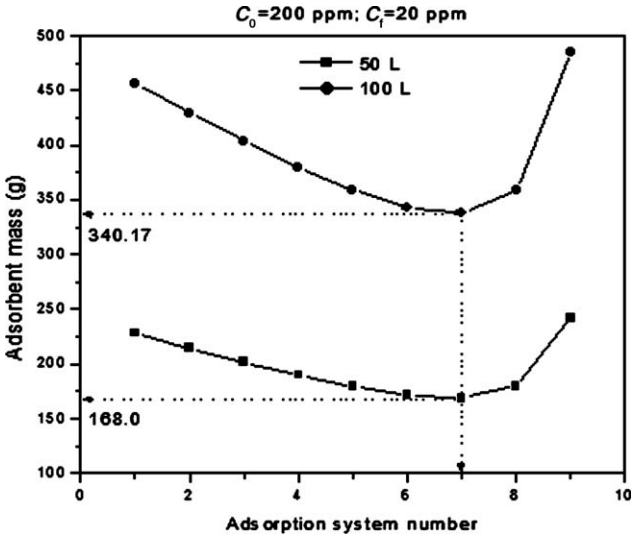

Figure 15. Two-stage adsorption system that requires minimum MIC(AA) dosage.

Table 11. Optimum Dose of MIC and MIC(AA) Required for the Treatment of Different Volumes of Metal Solutions (C_0 = 200 ppm; C_2 = 20 ppm)

Volume of Solution (L)	Dosage of Adsorbent (g)				% Saved	
	MIC		MIC(AA)			
	Stage 1	Stage 1 + 2 (Optimum)	Stage 1	Stage 1 + 2 (Optimum)	MIC	MIC (AA)
50	217.21	186.13	242.36	168.00	14.21	30.68
100	434.41	374.61	484.72	340.17	13.77	29.82

and active sites of the clay adsorbent because of acid activation. The adsorption isotherms were favorable because they were "concave down," which meant more metal uptake at low concentrations in the solution. Adsorption kinetics was of pseudo-second-order and the process was controlled by both intra-particle and film-diffusion. The clay adsorbent MIC being available abundantly in the Gulbarga region of Karnataka, India, and cost effective, it may prove economical for the removal of Pb(II) from wastewaters. From the two-stage batch adsorption system proposed using the experimental data; it was observed that the two-stage system reduced the adsorbent dose by about 14 and 30% of MIC and MIC(AA), respectively, when compared with that of single stage adsorption system.

Acknowledgments

Analytical services rendered by Sophisticated Test and Instrumentation Centre, Cochin University of Science and Technology, Kochi, Kerala, India, are gratefully acknowledged.

Notation

A_s = external surface area of adsorbent dose (cm^2)
A_w = specific surface area (m^2/g)
C_0 = initial concentration of Pb(II) in solution (mg/L)
C_e = equilibrium (residual) concentration of adsorbate in solution (mg/L)
C_f = final concentration of Pb(II) in adsorber (mg/L)
C_n = concentration in adsorber stage n (mg/L)
C_t = concentration of Pb(II) in solution at any time t (mg/L)
D = Dubinin-Radushkevich isotherm model constant (mol^2/J^2)
$\overline{D_p}$ = average particle diameter (m)
F = fractional attainment of equilibrium
I = intercept (mg/g)
k_1 = Lagergren's kinetic model rate constant (min^{-1})
k_2 = Ho's kinetic model rate constant (g/mg-min)
k_f = first-order rate constant (min^{-1})
k_s = second-order rate constant (L/mg-min)
k_{ip} = intra-particle diffusion rate constant (mg/g-$min^{0.5}$)
k_{fd} = film-diffusion rate constant (min^{-1})
k_e = external mass transfer coefficient (cm/s)
K_F = Freundlich adsorption model constant (L/g)
K_L = Langmuir adsorption model constant (L/mg)
K_{LF} = Sips model isotherm constant ($l/mg^{1/\gamma}$)
MIC = montmorillonite-illite clay
MIC(AA) = montmorillonite-illite clay (acid activated)
m = mass of adsorbent used in batch equilibrium adsorption studies (g)
n = Freundlich adsorption model exponent
N = Sips adsorption model exponent
q_e = amount of adsorbate [Pb(II)] adsorbed at equilibrium (mg/g)
q_m = monolayer adsorption capacity (mg/g)
q_t = amount of adsorbate [Pb(II)] adsorbed at any time t (mg/g)
R = universal gas constant (8.314 J/(gmol-K))
R_L = Langmuir separation factor
R^2 = correlation coefficient
T = absolute temperature (K)
t = time (min)
V = volume of solution (L)
v_p = volume of an adsorbent particle (m^3)
W = mass of adsorbent used in adsorber, (g)
ϕ = sphericity
ρ = density of adsorbent (kg/m^3)
χ^2 = chi-square

Literature Cited

1. Beena T, Chintan DC, Raksh VJ. Characterization of surface acidity of an acid montmorillonite activated with hydrothermal, ultrasonic and microwave techniques. *Appl Clay Sci*. 2006;31:16–28.
2. Mills GA, Holmes J, Cornelius EB. Acid activation of some bentonite clays. *J Phys Chem*. 1950;53:1170–1185.
3. Lo W, Chua H, Lam KH, Bi SH. A comparative investigation on the biosorption of lead by filamentous fungal biomass. *Chemosphere*. 1999;39:2723–2736.
4. World Health Organization. *Environmental Health Criteria -3: Lead*. Geneva: World Health Organization, 1977.
5. World Health Organization. *Guidelines for Drinking-Water Quality*, *vols*. 1 and 2.Geneva: World Health Organization, 1984.
6. Turan M, Mart U, Yuksel B, Celik MS. Lead removal in fixed-bed columns by zeolite and sepiolite. *Chemosphere*. 2005;60:1487–1492.
7. Potgieter JH, Potgieter-Vermaak SS, Kalibantonga PD. Heavy metals removal from solution by palygorskite clay. *Miner Eng*. 2006; 19:463–470.
8. Yadava KP, Tyagi BS, Singh VN. Effect of temperature on the removal of Pb(II) by adsorption on china clay and wollastonite. *J Chem Biotechnol*. 1991;51:47–60.
9. Singh AK, Singh DP, Singh VN. Removal of znic(II) from water by adsorption on china clay. *Environ Technol Lett*. 1988;9:1153–1162.
10. Srivastava SK, Tyagi R, Pal N. Studies on the removal of some toxic metal ions: part II. *Environ Technol Lett*. 1989;10:275–282.
11. Panday KK, Prasad G, Singh VN. Mixed adsorbents for Cu (II) removal from aqueous solutions. *Environ Technol Lett*. 1986;7:547–554.
12. Khan SA, Rehman R, Khan MA. Sorption of strontium on bentonite. *Waste Manage*. 1995;15:641–650.
13. Chakir A, Bessiere J, Kacemi KE, Marouf M. A comparative study of the removal of trivalent chromium from aqueous solutions by bentonite and expanded perlite. *J Hazard Mater*. 2002;95:29–46.
14. Chantawong V, Harvey NW, Bashkin VN. Comparison of heavy metal adsorptions by Thai kaolin and ball clay. *Water Air Soil Pollut*. 2003;148:111–125.
15. Onal M, Sarikaya Y, Alemdaroglu T. The effect of acid activation on some physicochemical properties of a bentonite. *Turk J Chem*. 2002;26:409–416.
16. Bureau of Indian Standards. *Activated Carbons, Powdered and Granular - Methods of Sampling and Test*, Bureau of Indian Standards, IS 877:1989.
17. Issabayeva G, Aroua MK, Sulaiman NMN. Removal of lead from aqueous solutions on palm shell activated carbon. *Bioresour Technol*. 2006;97:2350–2355.
18. Diaz FRV, Santos PS. Studies on the acid activation of Brazilian clays. *Quim Nova*. 2001;24:345–353.
19. McCabe WL, Smith JC, Harriott P.*Unit Operations of Chemical Engineering*, 7th ed. McGraw-Hill International Edition, Singapore, 2005.
20. Nayak PS, Singh BK. Instrumental characterization of clay by XRF, XRD and FTIR. *Bull Mater Sci*. 2007;30:235–238.
21. Freundlich H. Über die adsorption in lösungen. *Z Phys Chem*. 1907;57:385–470.
22. Langmuir I. The adsorption of gases on plane surfaces of glass, mica and platinum. *J Am Chem Soc*. 1918;40:1361–1403.
23. Dubinin MM, Radushkevich LV. Evaluation of microporous materials with a new isotherm. *Dokl Akad Nauk SSSR*. 1966;55:331–333.
24. Sips R. On the structure of a catalyst surface. *J Chem Phys*. 1948; 16:490–495.

25. Treybal RE. *Mass-Transfer Operations*, 3rd ed. Tokyo: McGraw-Hill, 1981.
26. Naseem R, Tahir SS. Removal of Pb(II) from aqueous/acidic solutions by using bentonite as an adsorbent. *Water Res.* 2001;35:3982–3986.
27. Lagergren S. Zur theorie der sogenannten adsorption gelöster stoffe. *K Sven Vetenskapsakad Handl.* 1898;24:1–39.
28. Ho YS, McKay G. Pseudo-second order model for sorption processes. *Process Biochem.* 1999;34:451–465.
29. Levenspiel O. *Chemical Reaction Engineering*. 3rd ed. Wiley, New York, 2008.
30. Weber Jr. WJ, Morris JC. Kinetics of adsorption on carbon from solution. *J Sanitary Eng Div Am Soc Civil Eng.* 1963;89 SA2:31–60.
31. Poots VJP, McKay G, Healy JJ. The removal of acid dye from effluent using natural adsorbents. I. Peat. *Water Res.* 1978;10:1061–1066.
32. McKay G, Otterburn MS, Sweeney AG. The removal of colour from effluent using various adsorbents-III. Silica: rate processes. *Water Res.* 1980;14:15–20.
33. Allen SJ, McKay G, Khader KYH. Intraparticle diffusion of a basic dye during adsorption onto sphagnum peat. *Environ Pollut.* 1989;56:39–50.
34. Kannan N, Sundaram MM. Kinetics and mechanism of removal of methylene blue by adsorption on various carbons—a comparative study. *Dyes Pigments.* 2001;51:25–40.
35. Ho YS, McKay G. Sorption of dye from aqueous solution by peat. *Chem Eng J.* 1998;70:115–124.
36. Srivastava VC, Swamy MM, Mall ID, Prasad B, Mishra IM. Adsorptive removal of phenol by bagasse fly ash and activated carbon: equilibrium, kinetics and thermodynamics. *Colloid Surface A.* 2006;272:89–104.
37. McKay G, Otterburn MS, Aga JA. Intraparticle diffusion process occurring during adsorption of dyestuffs. *Water Air Soil Pollut.* 1987;36:381–390.
38. Goswami S, Ghosh UC. Studies on adsorption behaviour of Cr(VI) onto synthetic hydrous stannic oxide. *Water SA.* 2005;31:597–602.
39. Morris JC, Weber WJ. *Removal of biologically-resistant pollutants from waste waters by adsorption*. In: Eckanfelder WW, editor. *Advances in Water Pollution Research*, *vol*. 2. London: Pergamon Press, 1964:231–266.
40. Boyd GE, Adamson AM, Myers LS. The exchange adsorption of ions from aqueous solutions by organic zeolites. II. Kinetics. *J Am Chem Soc.* 1949;69:2836–2848.
41. Noll KE, Gounaris V, Hou WS. *Adsorption Technology for Air and Water Pollution Control*. Chelsea, MI: Lewis, 1992.
42. Al-Duri B. *Introduction to Adsorption*. In: McKay G, editor. *Use of Adsorbents for the Removal of Pollutants from Wastewaters*. Boca Raton, FL: CRC Press, 1996:1–6.
43. Tsai WT, Chang CY, Ing CH, Chang CF. Adsorption of acid dyes from aqueous solution on activated bleaching earth. *J Colloid Interf Sci*. 2004;275:72–78.
44. Al-Degs YS, Tutunji MF, Baker HM. Isothermal and kinetic adsorption behaviour of Pb^{2+} ions on natural silicate minerals. *Clay Miner.* 2003;38:501–509.

Manuscript received Apr. 5, 2009, revision received Sept. 24, 2009, and final revision received Dec. 9, 2009.